CAIT-UTC-016

Highly Efficient Model Updating for Structural Condition Assessment of Large-Scale Bridges

Final Report
February 2015

Guirong (Grace) Yan
Assistant Professor
University of Texas at El Paso
El Paso TX 79912

Linren Zhou
South China University of Technology
Guangzhou 510641, China

External Project Manager
Charles Sikorsky
California Department of Transportation

In cooperation with
Rutgers, The State University of New Jersey
And
State of Texas
Department of Transportation
And
U.S. Department of Transportation
Federal Highway Administration

Disclaimer Statement

TECHNICAL REPORT STANDARD TITLE PAGE

1. Report No.	2. Government Accession No.	3. Recipient's Catalog No.
CAIT-UTC-016		

4. Title and Subtitle	5. Report Date
Highly Efficient Model Updating for Structural Condition Assessment of Large-Scale Bridges	February 2015
	6. Performing Organization Code CAIT/UTEP
7. Author(s) Guirong (Grace) Yan, Linren Zhou	8. Performing Organization Report No. CAIT-UTC-016
9. Performing Organization, Name and Address University of Texas at El Paso 500 W. University Avenue El Paso, TX 79912	10. Work Unit No.
	11. Contract or Grant No. DTRT12-G-UTC16
12. Sponsoring Agency Name and Address Center for Advanced Infrastructure and Transportation Rutgers, The State University of New Jersey 100 Brett Road Piscataway, NJ 08854	13. Type of Report and Period Covered Final Report 1/01/13 - 7/31/2014
	14. Sponsoring Agency Code

15. Supplementary Notes

U.S Department of Transportation/Research and Innovative Technology Administration
1200 New Jersey Avenue, SE
Washington, DC 20590-0001

16. Abstract

For efficiently updating models of large-scale structures, the response surface (RS) method based on radial basis functions (RBFs) is proposed to model the input-output relationship of structures. The key issues for applying the proposed method are discussed, such as selecting the optimal shape parameters of RBFs, generating samples by using design of experiments (DOE) and evaluating the RS model. The RS methods based on RBFs of Gaussian (GA), inverse quadratic (IQ), multiquadric (MQ) and inverse multiquadric (IMQ) are investigated. Results have demonstrated that RS methods based on RBFs can achieve a high approximation accuracy and better performance than the RS method based on polynomial function. The proposal method has been validated numerically and experimentally on a cable-stayed bridge model.

17. Key Words	18 Distributional Statement
Model Updating, Condition Assessment, Bridges	

19. Security Classification	20. Security Classification (of this page)	21. No. of Pages	22. Price
Unclassified	Unclassified	33	

Form DOT F 1700.7 (8-09)

Acknowledgments
The authors would like to thank U.S. Department of Transportation and Federal Highway Administration for their financial support, and to thank Rutgers, The State University of New Jersey and Dr. Soheil Nazarian from University of Texas at El Paso for their coordination.

Table of Contents

List of Figures

List of Tables

1. DESCRIPTION OF THE PROBLEM

During their lifetimes, bridges suffer from environmental corrosion, persistent traffic and wind loading, extreme earthquake events, and material aging, etc., which inevitably result in structural deficiencies. According to a recent report from the American Society for Civil Engineers, "more than 26%, or one in four, of the nation's bridges are either structurally deficient or functionally obsolete". Actually, a large percentage of the bridges in use in the United States have been used for several decades, maybe beyond their intended service lifetime. Therefore, their health condition should be assessed to ensure their integrity and to improve the safety for the public. The collapse of the I-35W highway bridge over the Mississippi River in Minneapolis (Minnesota, US, August 2007) further underscores the urgent need for reliable and robust condition assessment of bridges. A precise numerical model is very important for structural condition assessment (Adeli and Jiang, 2009; Hampshire and Adeli, 2000; Ou, 2004; Park, et al., 2007; Ou and Li, 2010; Xia, et al., 2011). However, it is difficult to develop a precise numerical model of a structure due to modeling simplification and modeling errors. Model updating provides an effective way to obtain a precise numerical model of a structure. Mottershead and Friswell (1993) presented a comprehensive literature review on model updating techniques.

When applying traditional model updating methods, an initial FEM of the structure is first established based on construction drawings and then numerous iterations are performed on the entire FEM during the optimization process, leading to a large amount of computation that is time-demanding and requires a lot of computational resources. The situation becomes much worse for large-scale real-world structures, in which a great number of degrees of freedom (DOFs) are involved and a great number of parameters on geometry, material properties as well as boundary conditions may need to be updated.

To alleviate this problem, the response surface (RS) method has been employed to generate an equivalent model (referred to as ‘surrogate model’) to replace the FEM in the model updating process (Fang and Perera, 2009; Faravelli and Casciati, 2004; Horta, 2010). The basic idea of the RS method is to model a structure by seeking an explicit function to approximate the implicit relationship between the physical parameters (input) and responses of the structure (output). The model established by the RS method is much more efficient in terms of computation amount and speed than the traditional FEM. The substitution model is referred to ‘meta-model’ or ‘surrogate model’ (Modak, et al., 2002).

Efforts have been witnessed for the RS method involved into FEM updating during the past ten years. Marwala (2004) proposed the RS method for structural model updating by using multilayer perception to approximate the relationship between system parameters and structural responses. Fang and Perera (2011) proposed a damage identification method achieved by response surface-based model updating using D-optimal designs. Lu Deng et al. (2010) updated a bridge model by using the genetic algorithm for optimization with the RS method for modeling the structure. The RS model was constructed by a quadratic polynomial (QP) function based on the experimental samples generated by central composite designs (CCD). Results of numerical simulations and the application of an existing bridge showed that this method worked well and achieved reasonable physical explanations for the updated parameters. When updating a bridge FEM, Ren et al. (2010, 2011) also employed the RS method based on quadratic polynomial functions to model the bridge. They pointed out that it is still challenging to apply the RS method in updating the models of complex civil engineering structures where the relationship between the design parameters and the output responses is complicated and a large number of updated parameters are involved. Through a comprehensive literature review in this area, the present authors found that almost all the reported researches about the RS method for model updating are based on polynomial functions, but that based on RBFs is not much studied, which is more suitable for multivariate and complicated problems. Recently, Qin et al. (2011) updated the FEM of airplane wing by using RS method of Gaussian function.

Through a comprehensive literature review, almost all the reported research in this area is based on polynomial functions, and is limited to simple structures. This project is to improve the RS method by applying a more appropriate approximation function (Radial basis function) and then perform a genetic algorithm on the surrogate model generated by the improved RS method to update models of large-scale bridges. As a result, the computational amount can be significantly reduced, making model updating more quickly. The implementation of the improved RS method makes model updating promising in being applied to large-scale real-world structures.

2. APPROACH AND METHODOLOGY

Various response surface (RS) methods will briefly reviewed in this section. The RS method as a comprehensive statistical and experimental technology has been widely used to predict the relationship between the input and output of complicated systems. It can also be considered as the function fitting or interpolation of the discrete data points, which obtains the numerical model of the concerned systems based on the observed samples in the design space. One feature of this method is to express a complicated implicit function using deterministic formulas. In this method, the approximate function is arguably considered as the most important factor. The polynomial function has been mostly used as it is continuously derivable and easy for subsequent computation.

2.1 The RS method based on polynomial functions

A polynomial function with different orders can be adopted as an approximate function in the RS method. The critical step is to properly determine the order and cross-terms of the polynomial function. For most problems, the first-order and second-order polynomial functions are usually used to satisfy modeling precision and achieve a reasonable amount of calculation (Hill, 1996). The most used second-order polynomial RS model can be expressed as

$$y = \beta_0 + \sum_{i=1}^{k} \beta_i x_i + \sum_{i=1}^{k} \beta_{ii} x_i^2 + \sum_{i<j} \sum_{j} \beta_{ij} x_i x_j + \varepsilon \tag{1}$$

Where *β* is the undetermined regression coefficient, *x* is the design variable, *k* is the number of design variables and *ε* is the error term.

The number of unknown coefficients *β* in second-order polynomial RS model is (k+1)(k+2)/2. *β* can be obtained by a least squares estimation. It should be noted that the number of undetermined coefficients of the polynomial RS model increase exponentially with the increase of design variables and the polynomial order, which means that more observed samples and larger calculation amount are required for the RS construction.

Theoretically, for simulation of complex problems such as a non-linear curved surface, the RS model with higher-order polynomial functions achieves better results. However, the number of unknown regression coefficients and the amount of calculation will subsequently increase significantly, making the cost of high-order RS model unacceptable, especially for multivariable problems.

2.2 The RS method based on RBFs

To overcome the disadvantages of the RS method base on polynomial function, the RS method based on radial basis functions (RBFs) is proposed in this section. RBFs were first proposed by Krige in 1951 in the Kriging method (Krige, 1951). They have been widely studied since 1950s and applied in many fields, such as geodesy, geophysics, surveying and mapping, photogrammetry, remote sensing, signal processing, geography, digital terrain modeling, hydrology (Hardy, 1990), solving elliptic, parabolic or hyperbolic partial differential equations (Fornberg and Piret, 2008), and RBF neural network (Adeli and Karim, 2000; Karim and Adeli, 2002, 2003; Ghosh, et al., 2008; Savitha, et al., 2009). In particular, the application of RBFs in the areas of function approximation and interpolation of scattered data has attracted considerable attention (Jackson, 1989). Compared with other approximate functions, RBFs can achieve a better performance and the advantage becomes more obvious for high-order nonlinear problems. RBFs have been validated to be the best one compared to other interpolation methods by using examples of different kinds of scattered data (Frank, 1982). Powell (1991) presented a good review of the theory of RBF approximation.

Radial basis function. The definition of RBF proposed by Stein and Weiss (1971) is as follows: if $\|x_1\| = \|x_2\|$, the function *ϕ* satisfying $\phi(x_1) = \phi(x_2)$ is a RBF. It means that the RBF only depends on the function $r = \|x\|$, where ||·|| denotes the Euclidean norm. The most commonly used RBFs are listed in Table 1, where *c* is the shape parameter and $r = \|x - x_i\|$ is the Euclidean norm.

Table 1 Commonly used RBFs

Name of RBF	*Expression*	*Abbreviation*
Gaussian	$\phi(r)=e^{-c\times r^2}\ (c>0)$	*GA*
Inverse Quadratic	$\phi(r)=(r^2+c^2)^{-1}$	*IQ*
Multiquadrtic	$\phi(r)=(r^2+c^2)^{1/2}$	*MQ*
Inverse Multiquadrtic	$\phi(r)=(r^2+c^2)^{-1/2}$	*IMQ*

Modeling of RS method based on RBFs. The RS method is to approximate a real-valued function $f(x)$ based on a finite set of values $f=\{f_1,\ldots,f_n\}$ at discrete points $X=\{x_1,\ldots,x_n\}\in R^d$. Herein RBFs are chosen to construct the RS model as an approximation of the function. For positive definite RBFs such as GA, IQ and IMQ functions, the RS model has the general form:

$$y=f(x)=\sum_{i=1}^{n}\lambda_i\phi(\|x-x_i\|)\quad (x\in R^d,\ x_i\in \mathrm{X}) \tag{2}$$

where $x=\{x^1,x^2,\cdots,x^k\}$ is the vector of design variables (k is the number of updating parameters); X is a given set of known discrete points, $\phi(r)=\phi(\|x-x_i\|)$ is a RBF; $\|x-x_i\|$ is the Euclidean distance between an arbitrary point x and a discrete point x_i; $\lambda=\{\lambda_1,\lambda_2,\cdots,\lambda_n\}$ is the regression coefficient vector of a RS model.

For conditional positive-definite RBFs such as MQ function, some additional polynomials and constraint conditions should be adopted for the modeling of RS model. The RS model takes the form

$$y=f(x)=\sum_{i=1}^{n}\lambda_i\phi(\|x-x_i\|)+\sum_{\alpha\le\gamma}b_\alpha x^\alpha \tag{3}$$

If $\alpha\ (\alpha\le\gamma)$ and $\sum_{i=1}^{n}\lambda_i x_i^\alpha=0$, the solution to Eq. (3) is unique. Where γ is the order of conditional positive-definite function; α and b_α are the order and regression coefficient of the additional polynomials, respectively.

As can be seen from Eqs. (2) and (3), the RS model based on RBFs can be described as a weighted sum of a radially symmetric basis function based on the Euclidean distance. It should be noted that the number of regression coefficients only depends on the observed points, and almost has no relationship with the dimension of the design variable vector x. Therefore, the increase of design parameters does not require more samples. As a result, the calculation efficiency can be improved and the computational cost significantly reduced, which is very important for high dimensional and multivariate problems.

Selection of the shape parameter c for RBFs. As shown in Table 1, the shape parameter c is the only undetermined coefficient in a RBF, which needs to be specified by the user. It controls the 'flatness' of RBFs, and is employed to adjust the curve shape of RBFs for achieving a better approximation precision.

The accuracy of approximating functions using RBFs highly depends on the selection of the shape parameter *c* (Frank, 1982; Carlson and Foley, 1991; Schaback, 1995). Therefore, selecting an appropriate shape parameter plays an important role when using RBFs. The value of the optimal *c* depends on the number and distribution of data points, the RBFs and the precision of the computation (the condition number of the interpolation matrix) (Rippa, 1999). The shape parameter *c* in RBFs application can be divided into constant *c* (Carlson and Foley, 1991) and variable *c* (Kansa and Carlson, 1992; Sarra and Sturgill, 2009). The variable *c*-based methods can produce more rational and accurate results. However, they are more complicated with high computational costs required. Therefore, the constant shape parameter-based methods have been widely used due to their simplicity and efficiency. In most cases, desired accuracy can be achieved with a constant shape parameter.

As a numerical illustration of the influence of the shape parameter *c* on function approximation, the Peaks function in MATLAB is adapted to be approximated by the RS method based on RBFs. Peaks is a bivariate function with the following form

$$z = f(x,y) = 3(1-x)^2 e^{-x^2-(y+1)2} - \\ 10(\frac{x}{5} - x^3 - y^5)e^{-x^2-y^2} - \frac{1}{3}e^{-(x+1)^2-y^2} \tag{4}$$

It is obtained by translating and scaling Gaussian distribution with three local minimum points and three local maximum points on the concave and convex continuous surface, as shown in Fig. 1(a). The RS models based on RBFs (GA and MQ) are developed for the Peaks function by using the proposed method as described in Subsection 2.2.2. Figures 1(b)-(d) display the errors distribution of the obtained RS approximation with different shape parameters *c* using the same set of data points. It is clear that the magnitude and distribution of approximation errors are obviously different from each other. If a small value *c*=0.5 is used, the major error distributes at the vicinity near edge where the surface is supposed to be flat. Using a large value *c*=10, the error concentrates around the maximum or minimum points of the surface. Using the value of *c*=1, a more uniform distribution and small errors are achieved. The above discrepancy is caused by the difference in the shape of the approximation function.

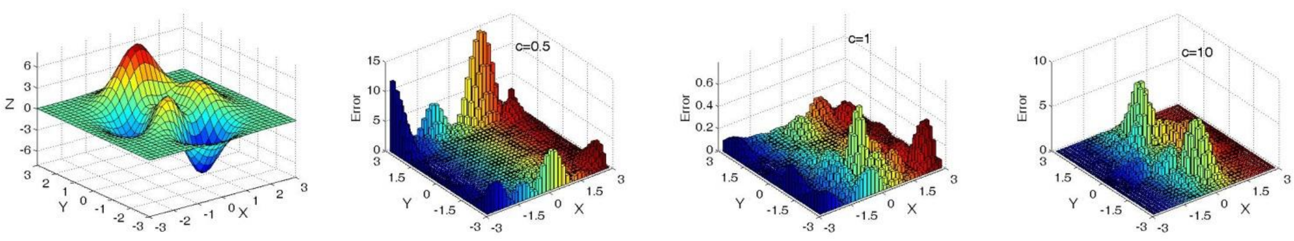

(a) The surface of Peaks (b) *c*=0.5 (c) *c*=1 (d) *c*=10

Fig. 1. The Peaks surface and the error distribution of the GA RS approximation (a) Peaks function, (b) *c*=0.5, (c) *c*=1 and (d) *c*=10

To investigate the influence of different RBFs and different numbers of samples on selecting the shape parameter *c*, the four RBFs were used to approximate the Peaks function with various amounts of samples. From Fig. 2, it can be observed that: 1) The approximation errors gradually change with the variation of the shape parameter *c*; 2) RBFs almost have the same minimum error, but the distribution of error is different; 3) As the number of the observed data points increases, the approximation error is reduced dramatically and a wider range of *c* can be used.

It can therefore be concluded that the selection of optimal *c* should take account of the approximation RBFs and properties of observed data points. It is suggested that a pre-analysis with different approximation functions and the shape parameter *c* as a continuous variable in a certain range is first conducted, and an optimal value of *c* can be obtained by observing the value and distribution of approximation errors. Before applying this approach to each individual bridge, *c* should be determined using the above instructions.

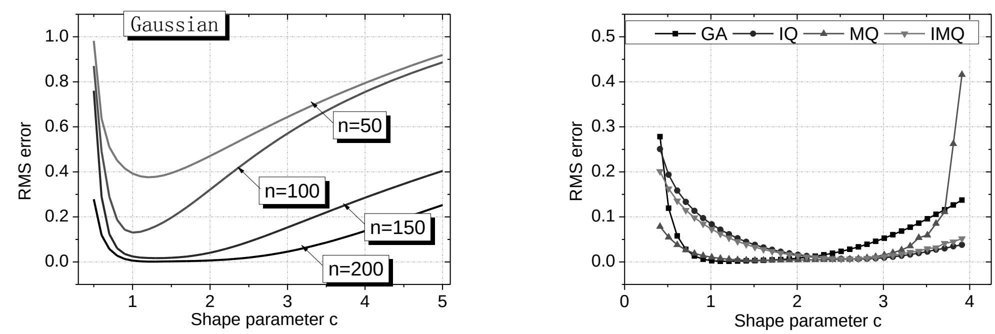

(a) GA function with various samples (b) Four RBFs with 200 samples

Fig. 2. RMS error as a function of *c* for the GA and MQ RS approximation defined on various amount of data points (*n* is the number of data points)

3. SAMPLING AND EVALUATION CRITERION OF THE RS METHOD

3.1. Sample generating based on design of experiment

The selection of samples is one of the key issues for the RS approximation, significantly affecting the accuracy and the computational cost of a RS to be constructed. Based on the mathematical statistics, design of experiment (DOE) can efficiently and reasonably choose the observed samples in the global design space. With the increase of model complexity, DOE has become an essential part of the modeling process. Numerous methods of DOE were developed for different proposes. Some methods were especially proposed for the RS method, such as Central Composite Design (CCD) (Montgomery, 2006), D-optimal design and Box-Behnken design of DOE.

The CCD is adopted in this study to generate samples. The CCD samples (assume n-factor) generally consist of three components: 1) Cube points. The 2^n cube points come from a two-level full factorial design, which takes the all possible combination of the two-level values of the parameters; 2) Axial points. The *2n* axial points are located on a hyper-cube with the radius α. An axial point is defined by the rule that one of the parameters has the minimum or maximum value and all other parameters have their mid-levels; 3) Center point. A single point in the center is created by a nominal design. The nominal design consists of one experiment where all parameters are set to their nominal values.

It should be noted that the samples for RS modeling and accuracy evaluation are different. When selecting samples for modeling, high computation efficiency and low experiment cost are required; when selecting the samples for accuracy evaluation, a uniform and random distribution in the design space of input parameters is required. In this study, the samples for RS modeling are generated by the CCD method, and uniformly distributed pseudo-random samples are utilized for precision evaluation.

3.2 Evaluation Criterion of the RS method

Many RS methods with different approximate functions and various optimization strategies are widely used in the engineering fields. Therefore, it is necessary that some evaluation criterions should be adopted to evaluate the validity and accuracy of the RS application, and the commonly used evaluation indexes are described in this section.

Multiple correlation coefficient R^2. The multiple correlation coefficient is used in a multiple regression analysis to assess the quality of the prediction of the dependent variable. It is an estimate of the combined influence of two or more input variables to the observed output quantity, expressed as

$$R^2 = \frac{SSR}{SSY} = \frac{\sum_{i=1}^{n}(\hat{y}_i - \bar{y})^2}{\sum_{i=1}^{n}(y_i - \bar{y})^2} \tag{5}$$

Only for a linear approximation, *SSR=SSY-SSE*, then R^2 can be further expressed as

$$R^2 = \frac{SSR}{SSY} = 1 - \frac{SSE}{SSY} = 1 - \frac{\sum_{i=1}^{n}(y_i - \hat{y}_i)^2}{\sum_{i=1}^{n}(y_i - \bar{y})^2} \tag{6}$$

Where n is the number of the observed samples; y_i is the observed value; $\bar{y}$ is the average value of y_i; and $\hat{y}_i$ is the predicted value by the RS model at observed points; *SSR* is the regression sum of squares which indicates the discreteness of y; *SSY* is the total sum of squares, showing the discreteness of y_i; *SSE* is the error of squared sum, indicating the discreteness of y caused by random errors.

The value of R^2 closer to 1 indicates that a higher accuracy of approximation is achieved. Usually, the $0.5 \le R^2 \le 0.8$ defines a significant correlation between dependent and independent variables and $0.8 \le R^2 \le 1.0$ means a high correlation. It should be noted that only for a linear approximation, the relationship of *SSR=SSY-SSE* can be obtained, then the R^2 in Eq. (6) is constrained in the range of [0, 1]. For more general problems of nonlinearity, the R^2 of Eq. (5) takes a value greater than 0.

Root mean squared (RMS) error. For approximation of a nonlinear function, precision can be evaluated appropriately by a RMS error, which can be written as

$$RMS = \sqrt{\frac{\sum_{i=1}^{n}(\hat{y}_i - y_i)^2}{n}} \quad (7)$$

A RMS error represents the discrepancy between measured values and predicted values of the RS model. A RS model with higher approximation accuracy achieves a smaller value of RMS error.

Obviously, the RMS error directly estimates the discrepancy between the measured value and prediction value, while the R^2 is an estimation of the correlation between dependent variables and independent variables. Compared with RMS, the R^2 has the advantage of comparing the accuracy of both diverse RS methods and different approximated problems in the range of 0~1, but cannot exactly explain the difference between each model. For example, when R^2 is close to 1, a small change of R^2 may generate a great discrepancy of RMS error. The precisions of different models can be reflected clearly by the RMS error, but it is inconvenient to have a comparative analysis for various models. In this study, both R^2 and *RMS* errors are adopted to estimate the accuracy of RS approximation.

4. FINDINGS

A cable-stayed bridge model (see Fig. 3) is used to illustrate the effectiveness of model updating using the RS method based on RBFs and Genetic Algorithm numerically and experimentally. The research findings are described as below.

4.1 Description of the structure

This bridge model was designed and manufactured according to the similarity theory based on a real-world bridge (Li, et al., 2006). The scale factor is 1/40. The bridge deck and towers were made of aluminum alloy, and cables were made of steel wires with different cross-sectional areas. The bridge deck is 15.2m long and 0.82m wide, and the middle pylon and side pylon are 3.1m and 1.9m high, respectively. The total weight of aluminum alloy is about 1 ton.

Fig. 3. Scaled model of a cable-stayed bridge

4.2 Establishing the RS model

To model the structure using the RS method, a three-dimensional finite element (FE) model of this bridge model was first developed using ANSYS, as shown in Fig. 4. The bridge girders, piers and towers were modeled by Element SOLID64, which have three translational degrees of freedom (DOFs) at each node. The bridge decks were modeled by Element SHELL63, which has both bending and membrane capabilities with six DOFs at each node (three translations and three rotations with respect to *x*, *y* and *z* directions). The bridge cables were simulated by LINK10 element, which has the unique feature of a bilinear stiffness resulting in a uniaxial tension-only (or compression-only) element.

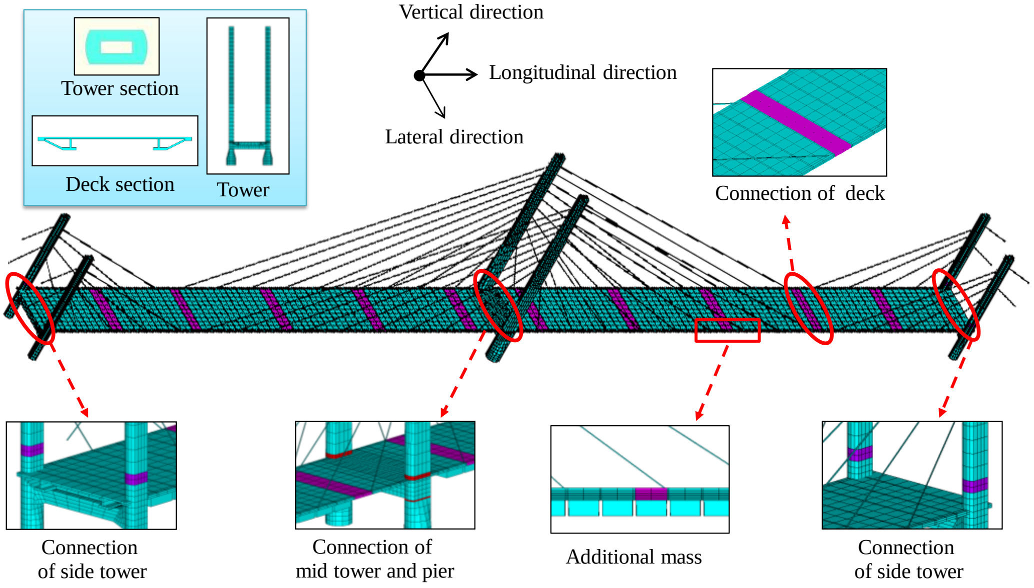

Fig. 4. FEM of the cable-stayed bridge model

4.2.1 Selection of the design parameters and output characteristic parameters

There exist discrepancies between the prototype bridge and the bridge model due to the differences in materials, dimensions, boundary conditions, and connections between segments. It is worth noting that it is very complicated and difficult to exactly depict the mechanical behaviors of the connections between segments. Therefore, the adjustments of the material properties of the connection elements are considered to simulate these discrepancies. A total of 10 design parameters with potential error are selected as input parameters for the RS modeling, which are listed in Table 2. Figure 4 shows the details of connection for FEM of the bridge model.

Here, the first 10 natural frequencies and MACs of mode shapes, as well as the tensions of 15 cables with different lengths and angles of inclination (see Fig. 4) are selected as the output characteristic parameters.

Table 2 Selected design parameters and baseline value

Parameters	*Baseline value*	*Notation*
Young's modulus of aluminum alloy of bridge decks and pylons	52 GPa	E1
Density of aluminum alloy of bridge decks and pylons	2700 kg/m^3	D1
Young's modulus of deck connection	52 GPa	E2
Young's modulus of pier connection	52 GPa	E3
Young's modulus of middle tower connection	52 GPa	E4
Young's modulus of side tower connection	52 GPa	E5
Mass of side tower connection	2700 kg/m^3	D2
Young's modulus of deck cables	200 GPa	E6
Young's modulus of boundary cables	200 GPa	E7
Density of deck additional mass	7850 kg/m^3	D3

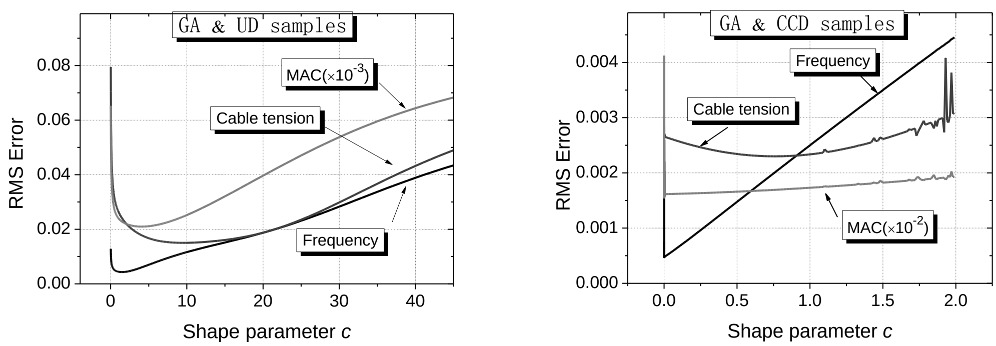

(a) GA function and samples of UD (b) GA function and samples of CCD

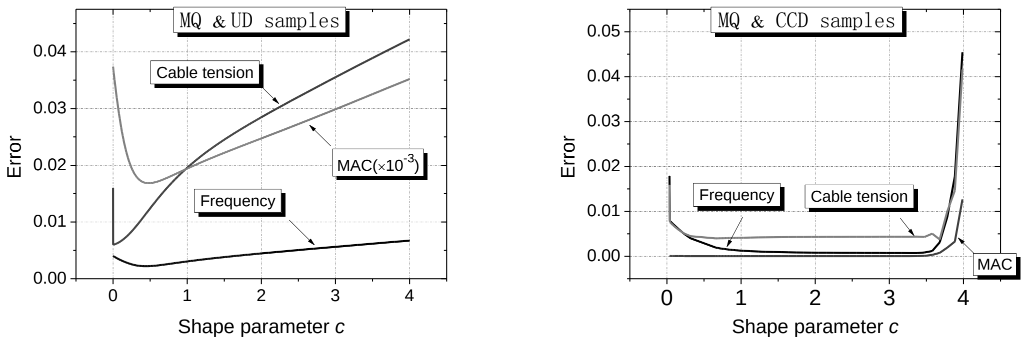

(c) MQ function and samples of UD (d) MQ function and samples of CCD

Fig. 5. The approximation error of RS model as a function of *c*

4.2.2 Selection of an optimal shape parameter c of RBFs for the RS method

To investigate the selection of optimal shape parameter *c* for RBF RS of approximating the implicit relationships between physical design parameters and static and dynamical output quantities of long-span cable-stayed bridge, the same numbers of CCD and uniform distribution samples, as well as GA and MQ functions for RS Model are discussed. Figure 5 shows the approximation RMS errors in different conditions with continuous variation of *c*, and the optimal *c* is defined as the value of *c* with the minimum approximation error.

It can be seen from Fig. 5 that the magnitude and distribution of approximation errors highly rely on the RBFs and observed samples. Most of the approximation errors have a continuous and smooth distribution. The error drops to a minimum and then increases with the *c* varies from zero to big value, and it is clear that an optimal *c* could be obtained when the error achieves to a minimum. However, it should be noted that there are some obvious discrepancies among them. The errors of RS approximation have different trends of distribution with respect to different characteristic quantities, samples and RBFs. Comparing Fig. 5(a) with Fig. 5(b) and Fig. 5(c) with Fig. 5(d), it shows that the error of UD samples smoothly changes and the minimum could be clearly found, but the error of CCD samples has more extreme changes when *c* takes an extremely small or relative big value. By observing the cable tension in Fig. 5(b), the error is dramatically disturbed when *c* takes a value near 2. One possible reason for the instability could be that the ill-conditioning occurs in calculation. By comparing Fig. 5(a) with Fig. 5(c) and Fig. 5(b) with Fig. 5(d), it can be seen that the GA and MQ RS model are similar with respect to UD samples, but the situation is obviously different for CCD samples. The MQ RS model based on CCD samples has a long stable region for optimal *c* and stability of solution.

4.2.3 Selection of RBFs

In this section, the performance of the RS method based on different RBFs is evaluated for approximation. For comparison, the RS method based on polynomial functions is also implemented. The flowchart of RS modeling and model updating based on RS methods of RBFs is shown in Fig. 6.

The CCD method is adopted to generate the samples for RS modeling. Level of center points takes the baseline value, and the corner points and star points take 120% and 80% of the baseline value as the upper and lower bounds, respectively. FE analysis is performed and corresponding characteristic quantities can be obtained from the output responses. Then, RS models are constructed based on input samples and the output characteristic quantities. Based on uniformly distributed pseudo-random samples, accuracy of RS approximation for each output quantity is investigated with the continuous change of c from 1.0×10^{-5} to 500, and the optimal c is determined when the error reached to the minimum. Meanwhile, the multiple correlation coefficient R^2 and RMS error are employed to evaluate the accuracy of RS methods. If the constructed RS models have good performance on both R^2 and RMS error, then they can be used for model updating. Otherwise, the observed samples and approximation function should be adjusted and the RS modeling procedures should be repeated.

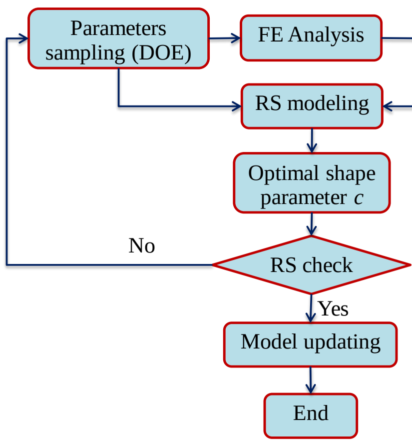

Fig. 6. The flowchart of RS modeling based on RBFs

Figure 7 presents the RS based on the GA function for the approximation of natural frequency, MAC and cable tension with respect to the design parameters of E1 and D1. It can be seen that the relationship between design parameters and MAC is more complicated than the other two.

The analysis of approximating precision. Figure 8 shows the R^2 and RMS error of the first 10 natural frequencies approximation of the five discussed RS models. As can be seen from Fig. 8(a), R^2 of all the five RS models are nearly equal to 1, which means that all the five RS models have high approximation quality of natural frequencies. The RMS error of the 10 natural frequencies is shown in Fig. 8(b), which clearly displays the detail precision of each RS models. It can be observed that the error has a stable distribution, and GA model has a higher accuracy than the other four RS models. QP (quadratic polynomial) model also has a good precision, but IQ, MQ and IMQ models have relative bigger errors. Focusing on the RBFs model, GA and IMQ have better accuracies than IQ and MQ.

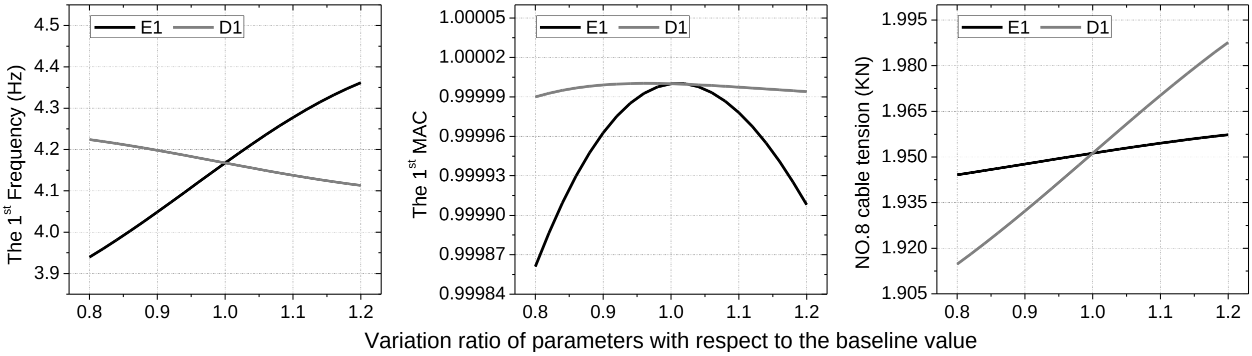

(a) The first natural frequency (b) The first MAC (c) The No. 8 cable tension

Fig. 7. GA RS of frequency, MAC and cable tension with respect to the design parameters of E1 and D1

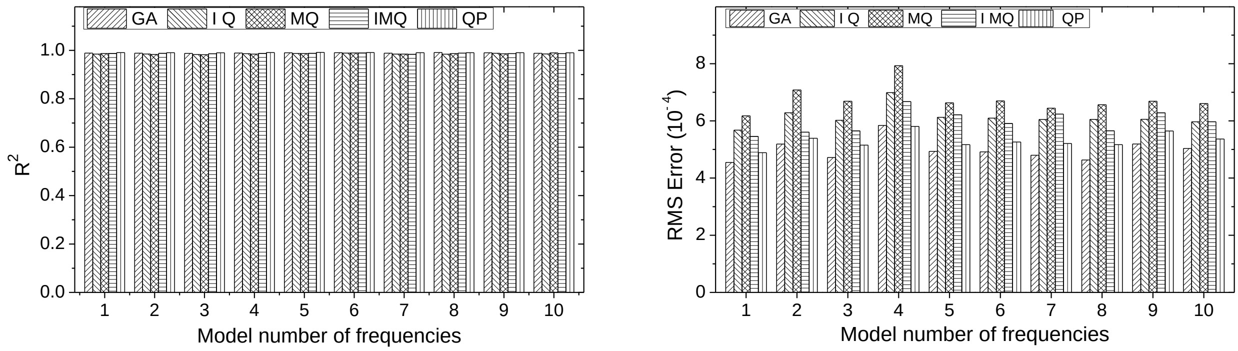

(a) The R^2 of frequencies (b) The RMS error of frequencies

Fig. 8. The RMS error and R^2 in the RS approximations of the first 10 frequencies

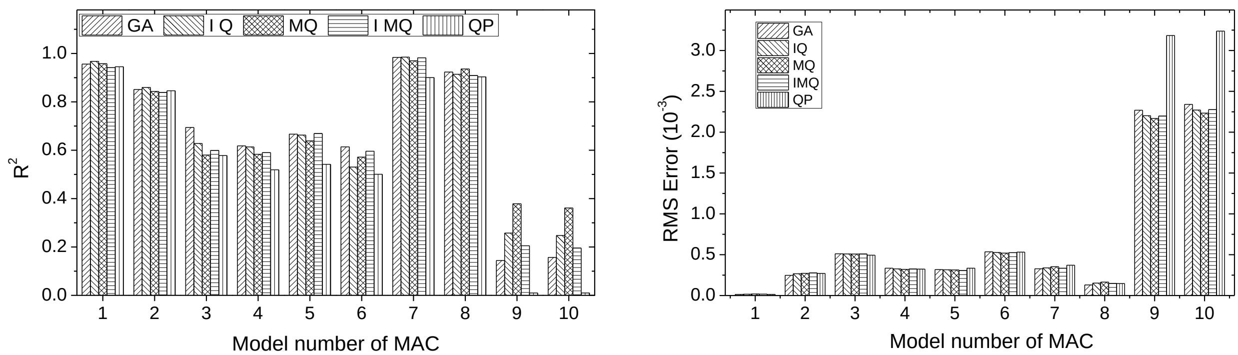

(a) The R^2 of MACs (b) The RMS error of MACs

Fig. 9. The R^2 and RMS error of the RS approximations for the first 10 MACs

Figure 9 presents the R^2 and RMS error of RS models approximation for the first 10 MACs. Clearly, the approximation results are not as good as natural frequencies, and RS models of RBFs have a relative better performance than QP model. The R^2 and RMS error for a different MAC change dramatically. As observed in Fig. 9(a), the RS approximations for MACs of the 9^{th} and 10^{th} are almost invalid. However, the other MACs have acceptable accuracies ($R^2 \geq 0.6$). It also could be seen in Fig. 9(b) that the RMS error of the 9^{th} and 10^{th} MAC are significantly bigger than other MACs. The 1^{st} MAC has the lowest error with an average value of 1.6×10^{-5}, but the 10^{th} MAC has the highest error with the mean value about 2.5.

There are two possible explanations for the high discreteness of MAC approximation. 1) MAC of mode shapes indicates the spatial vibration property of structure, the limit of measurement points in the experimental tests makes it difficult to capture the integral characteristic of the entire structure, especially for high-order mode shapes. Usually, only the first several mode shapes can be identified with a satisfied accuracy; 2) The mode shapes of a cable-stayed bridge are more complicated due to the flexibility of this type of structure and the coupling effect between the bridge deck and the tower.

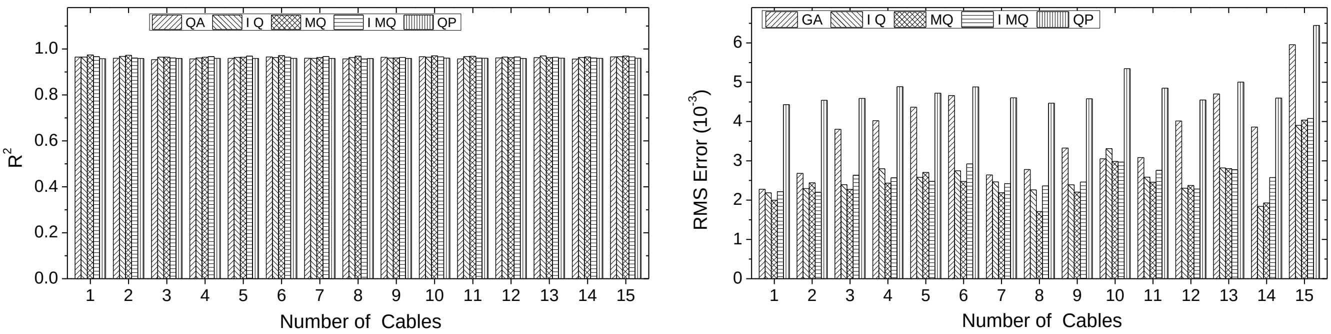

(a) The R^2 of cable tensions (b) The RMS error of cable tensions

Fig. 10. The RMS error and R^2 in the RS approximations of 15 different cable tensions

Figure 10 illustrates the R^2 and RMS error in RS approximation of 15 different cable tensions of the cable-stayed bridge. As shown in Fig. 10(a), all the R^2 are very close to 1, indicating that the quality of the approximations of RS methods to cable tensions is very good. The RMS errors are shown in Fig. 10(b), and it can be observed that the errors of the 15 cable tensions exhibit stationary distribution. Obviously, the RS method of RBFs has a better performance than the QP method; MQ and IMQ of RBFs could obtain a higher accuracy than the GA and IQ model.

Multiple correlation coefficient R^2 is used to assess the quality of RS approximation by correlation between design parameters and response quantities. A RMS error directly estimates the gap between the observed points and the approximation value of RS method. However, R^2 and RMS error may not reach a consistent conclusion. Since R^2 and RMS error are both very important evaluation indices for RS method approximation, it is suggested that only the RS method approximation with good performance in both R^2 and RMS error should be utilized for model updating.

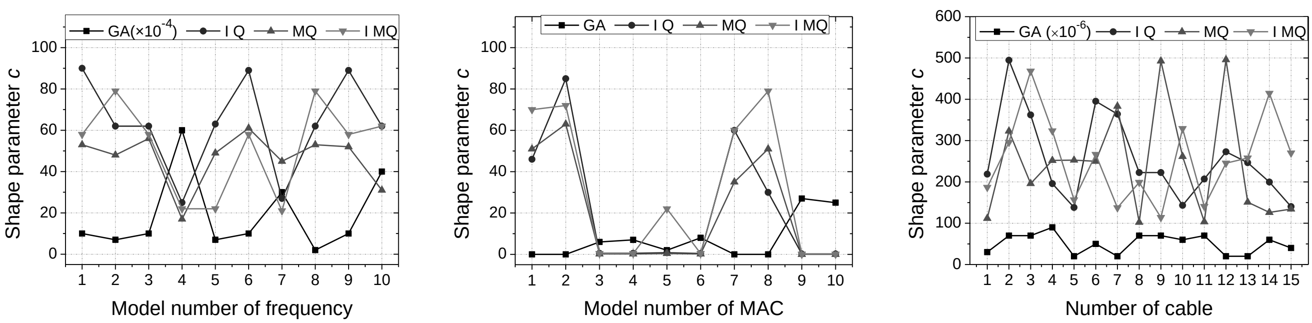

(a) Frequencies (b) MACs (c) Cable tensions

Fig. 11. Optimal shape parameter c in the RS approximations of frequencies (a), MACs (b) and cable tension (c)

***The optimal shape parameter c*.** The optimal shape parameter *c* for each RS model with respect to approximated characteristic quantity is determined independently. Precision inspection is conducted repeatedly with the *c* monotonously and continuously changing from 0 to 500 and the optimal *c* is determined when the approximation error drops to the minimum. Figure 11 illustrates the selected optimal *c* in the RS model of RBFs approximation to natural frequencies, MACs and cable tensions. It can be seen that the optimal *c* changes irregularly and highly depends on RBFs and approximated characteristic quantities. From Figs. 11(a)-(c), the optimal *c* of RBFs for different natural frequencies and cable tensions approximation changes stably, but MACs exhibit extreme situations where the optimal *c* takes a value that is close to 0 or a big value.

The above analysis indicates that for approximating the system of large and complex structure by using the RS method of RBFs, the optimal *c* highly depends on the approximated problems and should be determined independently. The approach of precision inspection with *c* as a continuously variable in a reasonable range is recommended, and then the optimal *c* can be determined as the approximation error reaches to the minimum. Normally, for an individual bridge, the responses measured from this bridge are quite similar to each other. The selected *c* and RBFs should be applied to all sets of data measured from this bridge.

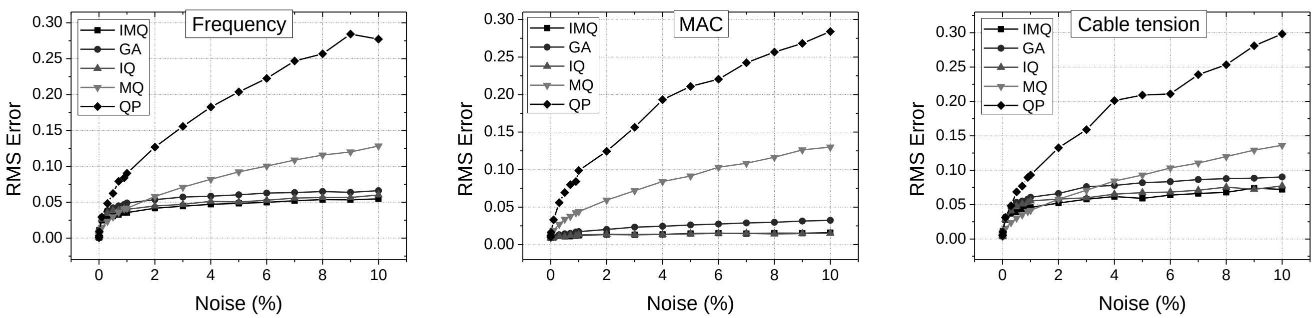

(a) Frequency (b) MAC (c) Cable tension

Fig. 12. Approximation error of RS models for frequency (a), MAC (b) and cable tension (c) under the situation of data contaminated by different degree noise

4.3 Model updating results

Dynamic testing has been conducted on the bridge model and the experimental setup is shown in Fig. 13. The accelerometers are installed on both sides of the bridge deck along the longitudinal direction. There are totally 18 measurement points with symmetric distribution (14 points for vertical testing and the other 4 points for lateral testing). Two electromagnetic shakers are installed at the closure segments to excite the bridge model using white noise excitation.

Table 3 Identified natural frequencies *(Hz)*

Order	*Description*	*Value*

1	The first order of vertical mode	4.014
2	The second order of vertical mode	8.839
3	The third order of vertical mode	10.822
4	The first order of lateral mode	10.963
5	The fourth order of vertical mode	11.857
6	The fifth order of vertical mode	14.312
7	The second order of lateral mode	15.075
8	The sixth order of vertical mode	16.344
9	The seventh order of vertical mode	21.926
10	The eighth order of vertical mode	22.962

Based on the dynamic testing, the first ten natural frequencies (see Table 3) of the bridge deck are identified by eigen-system realization algorithm (ERA) combined with natural excitation technique (NExT). ERA and NExT methods for modal parameters identification have been widely used in the field testing and lab experiment of civil engineering structures.

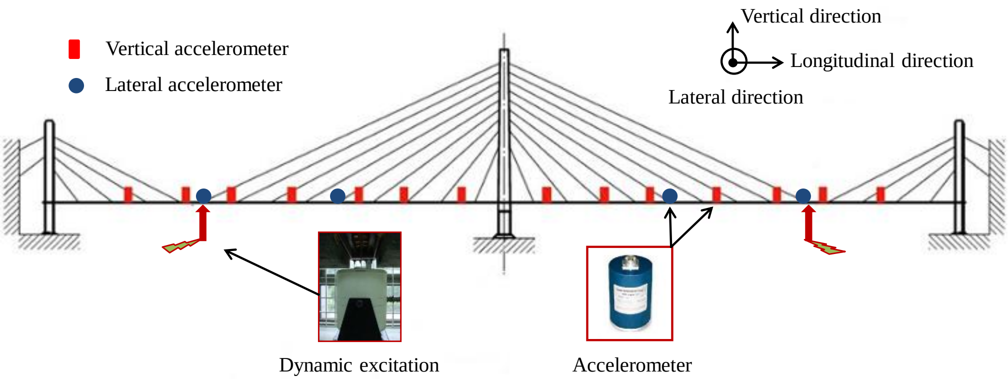

Fig. 13. Dynamic testing of the bridge physical model

A cable-stayed bridge is taken as simulation study and experiment validation to demonstrate and present the procedures of the proposed RS method based on RBFs for FEM updating. According to the manufacture of the bridge physical model and limited dynamic testing data for model updating, six parameters with potential errors are selected to be updated in the model updating. They are Young's modulus of aluminum alloy (E1), density of aluminum alloy (D1), Young's modulus of deck connections (E2), the additional mass on deck (D3), Young's modulus of deck cables (E6), Young's modulus of boundary cables (E7). Their baseline values are 52 GPa, 2700 kg/m^3, 52 GPa, 51 kg, 200 GPa and 200 GPa, respectively. The baseline values are usually chosen from the original construction drawings of structures. The sensitivities of the first ten frequencies with respect to the selected six physical parameters are shown in Fig.14. It can be seen that all six parameters have considerable influence on natural frequencies, but E2 has a relatively small sensitivity compared with the other parameters.

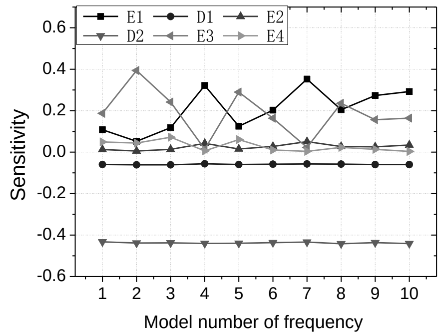

Fig. 14. Sensitivity of frequencies to physical parameters

The physical parameters are sampled by using CCD of DOE. The initial design value of each parameter is taken as the level of center points in CCD sampling, and the corner points and star points take the levels of 120% and 80% of the initial value, respectively. Then, the axial points of six-parameter CCD samples take the values of 52.43% and 147.57% of initial value. A total of 45 samples are used for RS modeling. The FEM analysis is implemented with the samples of parameters as input, and the corresponding response of natural frequencies are obtained. Then, the RS model of each natural frequency is constructed by the RS method based on GA function. GA RBF is used for the RS modeling because it has a good performance on approximating the relationships between natural frequencies and physical parameters as discussed in Section 4.4.

Table 4 Optimal shape parameter *c*

Freq. No.	1	2	3	4	5	6	7	8	9	10
Optimal c (10^{-4})	8.3	7.5	8.6	8.9	6.5	8.3	5.7	6.9	8.7	6.9

Accuracies of RS approximation of the ten natural frequencies are investigated with the continuous change of shape parameter c from 1.0×10^{-5} to 10, and the optimal c is determined when the error reaches to the minimum. The optimal c for the RS models of frequencies is listed in Table 4. The multiple correlation coefficient R^2 and RMS error are employed to evaluate the constructed RS models as shown in Fig. 15. It can be seen that all the R^2 are very close to 1 and the RMS errors are very small (10^{-5}), then it can be concluded that the RS models have good quality and accuracy of approximation, and can be used for the following model updating.

4.3.1 Model updating results based on numerical simulation data

Numerical simulation of model updating on the bridge model is carried out to test the validity of the proposed approach. A random change is taken to the physical parameters based on the initial design values in design space and corresponding natural frequencies are obtained from the FEM analysis as target (measured) characteristic information for model updating. An objective function is built up using the residuals between the measured and the RS predicted natural frequencies

$$Obj(X)=\sum_{i=1}^{N} w_i \left(\frac{f_{ai}-f_{ei}}{f_{ei}} \right)^2 \tag{8}$$

where f_{ei} and f_{ai} are the ith measured and RS predicted natural frequencies respectively; w_i is the weight coefficient of ith natural frequency; N is the number of modes involved and X is the vector of design parameters.

Then, FEM updating is implemented based on the constructed RS models and objective function (values of all the weight coefficients are taken as 1) by using a genetic algorithm (Sgambi, et al., 2012; Putha, et al., 2012). The updated results of numerical simulation are summarized in Table 5. The updated values of the parameters are very close to the true values with a maximum error of only 0.91%. The comparison of the 10 natural frequencies which are employed for model updating can be found in Table 6. The updated values and true values of natural frequencies are almost the same. Therefore, the numerical simulation indicates that the performance of the RS method of RBFs for model updating of cable-stayed bridge is very encouraging.

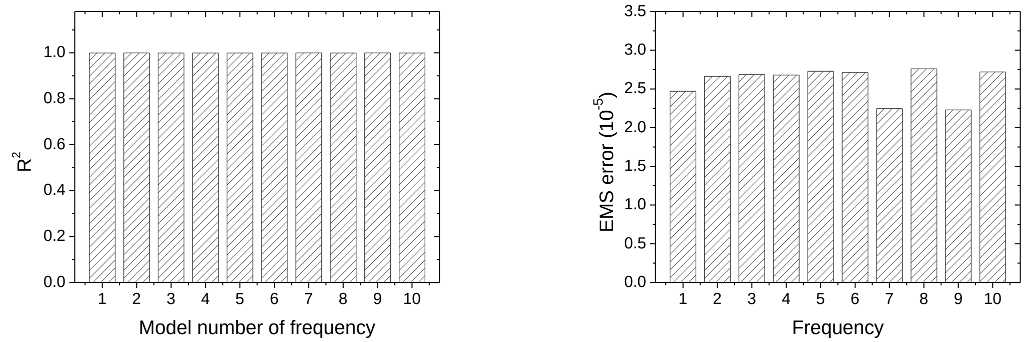

(a) Multiple correlation coefficient R^2 (b) Root mean squared (RMS) error

Fig. 15. R^2 and RMS errors of the GA RS models of natural frequencies

Table 5 Model updating results of cable-stayed bridge in numerical simulation

Parameters	*Notation*	*Initial value*	*Target value*	*Updated value*	*Error (%)*
Young's modulus of aluminum alloy (GPa)	E1	52	49.92	49.95	0.06
Density of aluminum alloy (kg/m^3)	D1	2700	2835.00	2832.84	-0.08
Young's modulus of deck connection (GPa)	E2	52	44.20	44.61	0.91
The additional mass on deck (kg/m^3)	D3	7850	8007.00	7991.61	-0.19
Young's modulus of deck cables (GPa)	E6	200	190.00	190.22	0.12
Young's modulus of boundary cables (GPa)	E7	200	180.00	180.70	0.39

Table 6 Comparison of natural frequencies after model updating in numerical simulation

Order	*Target value (Hz)*	*Updated value (Hz)*	*Error (%)*
1	4.0349	4.0350	0.0015
2	8.9033	8.9038	0.0051
3	10.8117	10.8121	0.0038
4	11.6142	11.6129	-0.0114
5	11.6060	11.6045	-0.0134
6	14.0175	14.0174	-0.0006
7	14.8664	14.8684	0.0137
8	15.5512	15.5523	0.0071
9	21.0115	21.0133	0.0087
10	21.5404	21.5368	-0.0167

4.3.2 Model updating results based on experimental data

Model updating is also carried out on the bridge model based on experimental data. The objective function is built up using Eq. (8). The weight coefficients of the objective function are taken as [3 3 3 1 2 2 2 1 1 1] for the first ten natural frequencies. The lower order natural frequencies take relative larger weight coefficients than higher natural frequencies because the lower natural frequencies of structures can be identified with high accuracy, and lateral model (4^{th} mode) of bridge deck takes a small weight coefficient because the testing and identification are not much reliable due to the fact that few sensors are used. Model updating is optimized by using a genetic algorithm. The lower and upper bounds for the six parameters are set to be [90%; 90%; 60%; 90%; 90%; 60%] and [105%; 105%; 100%; 105%; 105% 110%] of initial design values.

Table 7 Results of model updating based on experimental data

Parameter	*Initial value*	*Updated value*	*Difference (%)*
E1 (GPa)	52	50.76	-2.39
D1 (kg/m^3)	2700	2772.90	2.70
E2 (GPa)	52	45.77	-11.99
D3 (kg/m^3)	7850	7930.07	1.02
E6 (GPa)	200	194.58	-2.71
E7 (GPa)	200	157.00	-21.50

The results of model updating are listed in Table 7. As can be seen from the table, the Young's modulus of aluminum alloy (E1) and the additional mass on deck (D3) have been decreased because the material and dimension are slightly smaller than real values. The increase of the density of aluminum alloy (D1) is reasonable because of the connections of deck and cables increase the mass on the deck. The large decrease of Young's modulus of deck connection (E2) can be predictable because the stiffness of the connection of deck is weaker than the intact deck. The decrease in Young's modulus of deck cables (E6) and boundary cables (E7) could be attributed to the weakness of the connection and boundary condition at the end of cables.

Table 8 Error of natural frequencies after model updating based on experimental data

Order	*Measured value (Hz)*	*Updated value (Hz)*	*Error (%)*
1	4.014	4.045	0.760
2	8.839	8.971	1.493
3	10.822	10.824	0.022
4	10.963	11.722	6.922
5	11.857	11.662	-1.648
6	14.312	14.167	-1.012
7	15.075	15.033	-0.280
8	16.344	15.722	-3.806
9	21.926	21.247	-3.096
10	22.962	21.830	-4.932

The comparison of the natural frequencies between measured values and updated values after model updating can be seen from Table 8. The results are acceptable with almost all errors below 5% except the first-order lateral mode with the largest error 6.92%. However, it is obvious that the results are not so good as numerical simulation. The gap between tested values and updated values cannot be closed because of the existing error in testing and identifying of the physical model experiments. The relatively big errors in lateral modes and higher order modes are consistent with the practical cases in field testing.

As shown in Sections 4.3.1 and 4.3.2, the proposed approach can obtain structural physical parameters at any time instant by performing model updating. If structural physical parameters associated with time instants are obtained, structural condition change can be easily identified by comparing the obtained two sets of data. Of course, the change in the updated parameters (such as young's modulus here) may not express the condition change in the same way as visual inspection, such as "Good", "Fair" or "Bad". The relationship between the change in young's modulus and the change in structural condition should be further investigated.

The condition change in elements can be reflected from the change in Young's modulus of material for the elements or from changes in some other physical parameters. If changes in boundary conditions affect elements, for example a relatively loose connection between a cable and the deck may reduce the pretension in the cable, this condition change can be detected by the reduction of Young's modulus of the cable.

5. CONCLUSIONS

This project proposed the RS method based on RBFs to model large-scale structures for model updating. The complicated and implicit relationships between design parameters and output characteristic parameters of cable-stayed bridges are employed to investigate the performance of the RS method based on RBFs. A three-dimensional finite element (FE) model of a scaled cable-stayed bridge model is established for numerical simulation. The design parameters of interest include global and local physical parameters, and the output response quantities consist of static and dynamic characteristics of cable-stayed bridges.

Numerical simulation results on a cable-stayed bridge show that all of the RS models have high accuracy for approximation of natural frequencies, MACs and cable tensions, and a RS model of RBFs exhibits a better performance than a RS model based on polynomial. In particular, RBF based on GA has the highest precision for approximation of natural frequencies, but RBFs based on MQ and IMQ have a better accuracy for approximation of cable tension.

It is demonstrated that the increase of design space dimensions (model variables) does not require more samples for RBF RS construction. Therefore, the RS method based on RBFs has the potential to apply in more complicated, high dimensional and multivariate problems. The approach and strategies proposed in this project has been applied to model updating of a cable-stayed bridge model. Numerical simulation and experimental results indicate that the proposed method works well and can be easily implemented in practice for model updating of complicated bridges such as long-span cable-stayed bridges.

RECOMMENDATIONS

To successfully apply the RS method of RBFs for model updating of cable-stayed bridges, appropriate RBF for different approximated relationship should be firstly determined. Meanwhile, the selection of an optimal c of RBFs is very important, which heavily depends on the modeling samples, the type of RBFs and the approximated relationship. Before the proposed approach is implemented to real-world bridges, experimental validation on an actual bridge should be performed.

REFERENCES

Adeli, H. & Jiang, X. (2006), Dynamic fuzzy wavelet neural network model for structural system identification, *Journal of Structural Engineering*, 132(1), 102–111.

Adeli, H. & Jiang, X. (2009), *Intelligent Infrastructure – Neural Networks, Wavelets, and Chaos Theory for Intelligent Transportation Systems and Smart Structures*, CRC Press, Taylor & Francis, Boca Raton, Florida USA.

Adeli, H. & Kim, H. (2009), *Wavelet-Based Vibration Control of Smart Buildings and Bridges*, CRC Press, Taylor & Francis, Boca Raton, Florida, USA.

Adeli, H. & Karim, A. (2000), Fuzzy-Wavelet RBFNN Model for Freeway Incident Detection, *Journal of Transportation Engineering*, 126(6), 464–471.

Carlson, R.E. & Foley, T.A. (1991), The parameter R^2 in multiquadric interpolation, *Computers & Mathematics with Applications*, 21(9), 29–42.

Deng, L. & Cai. C.S. (2010), Bridge model updating using response surface method and genetic algorithm, *Journal of Bridge Engineering*, 15(5), 553–564.

Fang, S. E. & Perera, R. (2009), A response surface methodology based damage identification technique, *Smart Materials and Structures*, 18(6), 1–14.

Fang, S.E. & Perera, R. (2011), Damage identification by response surface based model updating using D-optimal design, *Mechanical Systems and Signal Processing*, 25(2),717–733.

Faravelli, L. & Casciati, S. (2004), Structural damage detection and localization by response change diagnosis, *Structural Safety and Reliability*, 6(2), 104–115.

Fornberg, B. & Piret, C. (2008), On choosing a radial basis function and a shape parameter when solving a convective PDE on a sphere, *Journal of Computational Physics*, 227 (2008), 2758–2780

Franke, R. (1982), Scattered data interpolation: test of some methods, *Mathematics of Computation*, 1982, 38(157), 181–200.

Gangone, M.V., Whelan, M.J. & Janoyan, K.D. (2011), Wireless Monitoring of a Multi-Span Bridge Superstructure for Diagnostic Load Testing and System Identification, *Computer-Aided Civil and Infrastructure Engineering*, 26(7), 569–579.

Ghosh-Dastidar, S., Adeli, H. & Dadmehr, N. (2008), Principal Component Analysis-Enhanced Cosine Radial Basis Function Neural Network for Robust Epilepsy and Seizure Detection, *IEEE Transactions on Biomedical Engineering*, 55(2), 512-518.

Hampshire, T.A. & Adeli, H. (2000), Monitoring the behavior of steel structures using distributed optical fiber sensors, *Journal of Constructional Steel Research*, 53(5), 267–281.

Hardy, R.L. (1990), Theory and applications of the multiquadric -biharmonic method, *Computers & Mathematics with Applications*, 19 ,163–208.

Hill, W.J. & Hunter, W.G. (1966), A review of response surface methodology: a literature survey, *Technometrics*, 8 (4), 571–590.

Horta, L.H., Reaves, M.C., Buehrle, RD., Templeton, J.D., Lazor, D.R., Gaspar, J.L., Parks, R.A. & Bartolotta, P.A. (2010), Finite Element Model Calibration Approach for Ares I-X, *Proceedings of IMAC XXVIII*, Jacksonville, Florida, USA, pp.1037-1054.

Jackson, I.R.H .(1989), *Radial basis functions: a survey and new results*, The Mathematics of Surfaces, III, Oxford University Press, Oxford, UK.

Jafarkhani, R. & Masri, S.F. (2011), Finite element model updating using evolutionary strategy for damage detection, *Computer-Aided Civil and Infrastructure Engineering*, 26(3), 207–224.

Jiang, X. & Adeli, H. (2005), Dynamic wavelet neural network for nonlinear identification of highrise buildings, *Computer-Aided Civil and Infrastructure Engineering*, 20(5), 316–330.

Jiang, X. & Adeli, H. (2007), Pseudospectra, MUSIC, and dynamic wavelet neural network for damage detection of highrise buildings, *International Journal for Numerical Methods in Engineering*, 71(5), 606–629.

Jiang, X. & Adeli, H. (2008a), Dynamic fuzzy wavelet neuroemulator for nonlinear control of irregular highrise building structures, *International Journal for Numerical Methods in Engineering*, 74(7), 1045–1066.

Jiang, X. & Adeli, H. (2008b), Neuro-Genetic algorithm for nonlinear active control of highrise buildings, *International Journal for Numerical Methods in Engineering*, 75(7), 770–786.

Jiang, X., Mahadevan, S. & Adeli, H. (2007), Bayesian wavelet packet denoising for structural system identification, *Structural Control and Health Monitoring*, 14(2), 333–356.

Kansa, E.J. & Carlson, R.E. (1992), Improved accuracy of multiquadric interpolation using variable shape parameters, *Computers & Mathematics with Applications*, 24(12): 99–120.

Karim, A. & Adeli, H. (2002), Comparison of fuzzy-wavelet radial basis function neural network freeway incident detection model with california algorithm, *Journal of Transportation Engineering*, 28(1), 21–30.

Karim, A. & Adeli, H. (2003), Radial basis function neural network for work zone capacity and queue estimation, *Journal of Transportation Engineering*, 129(5), 494–503.

Khuri, A.I. & Cornell, J.A. (1987), *Response surface designs and analysis*. Marcel Dekker, Inc., New York, N. Y., USA.

Krige, D.G. (1951), A statistical approach to some basic mine valuation problems on the Witwatersrand, *Journal of the Chemical, Metallurgical and Mining Society of South Africa*, 52,(6), 119–139.

Li, H., Huang, Y., Chen, W.L., Ma, M.L., Tao, D.W. & Ou, J.P. (2011), Estimation and warning of fatigue damage of FRP stay cables based on acoustic emission technique and fractal theory, *Computer-Aided Civil and Infrastructure Engineering*, 26(7), 500–512.

Li, H., Huang, Y., Ou, J. & Bao, Y. (2011), Fractal dimension-based damage detection method for beams with a uniform cross-section, *Computer-Aided Civil and Infrastructure Engineering*, 26(3), 190–206.

Li, H., Ou, J. & Zhao, X. (2006), Structural health monitoring system for the Shandong Binzhou Yellow River Highway Bridge, *Computer-Aided Civil and Infrastructure Engineering*, 21(4), 306–317.

Marwala, T. (2004), Finite element model updating using response surface method. Collection of Technical Papers - *AIAA/ASME/ASCE/AHS/ASC Structures, Structural Dynamics and Materials Conference*, vol. 7, pp.5165–5173.

Modak, S.V., Kundra, T.K. & Nakra, B.C. (2002), Comparative study of model updating methods using simulated experimental data, *computers & structures*, 80(5-6), 437–447.

Montgomery, D.C. (2006), *Design and analysis of experiments*, John Wiley & Sons, Inc., New York, N. Y., USA.

Mottershead, J.E. & Friswell, M.I.(1993), Model updating in structural dynamics: a survey, *Journal of Sound and Vibration*, 167(2), 347–375.

Ou J.P. (2004), Advances on vibration control and health monitoring of civil infrastructures in mainland China, *International Symposium on Network and Center-Based Research for Smart Structures Technologies and Earthquake Engineering*. Tokyo, Japan, pp.6–10.

Ou, J.P. & Li H. (2010), Structural health monitoring in mainland China-review and future trends, *Structural Health Monitoring*, 9(3), 219–231.

Park, H. S., Lee, H.M. & Adeli, H. (2007), A new approach for health monitoring of structures: terrestrial laser scanning, *Computer-Aided Civil and Infrastructure Engineering*, 22(1), 19–30.

Powell. M.J.D. (1991), *The theory of radial basis function approximation in 1990*, Oxford University Press, Oxford, UK.

Putha, R., Quadrifoglio, L. & Zechman, E. (2012), Comparing ant colony optimization and genetic algorithm approaches for solving traffic signal coordination under oversaturation conditions, *Computer-Aided Civil and Infrastructure Engineering*, 27(1), 14–28.

Qiao, L., Esmaeily, A. & Melhem, H.G. (2012), Signal pattern-recognition for damage diagnosis in structures, *Computer-Aided Civil and Infrastructure Engineering*, 27(9) 699–710.

Qin, Y., Kong, X. & Luo, W. (2011), Finite element model updating of airplane wing based on Gaussian radial basis function response surface, *Journal of Beijing University of Aeronautics and Astronautics*, 37(11). 1465–1470.

Ren, W.X. & Chen, H.B. (2010), Finite element model updating in structural dynamics by using the response surface method, *Engineering Structures*, 32(8), 2455–2465.

Ren, W.X., Fang, S.E. & Deng, M.Y. (2011), Response surface based finite element model updating using structural static responses, *Journal of Engineering Mathematics*, 137(4), 248–257.

Rippa, S. (1999), An algorithm for selecting a good value for the parameter e in radial basis function interpolation, *Advances in Computational Mathematics*, 11(2), 193–210.

Sarra, S.A. & Sturgill, D. (2009), A random variable shape parameter strategy for radial basis function approximation methods, *Engineering Analysis with Boundary Elements*. 33(11), 1239–1245.

Savitha, R., Suresh, S. & Sundararajan, N. (2009), A fully complex-valued radial basis function network and its learning algorithm, *International Journal of Neural Systems*, 19(4), 253–267.

Schaback, R. (1995), Error estimates and condition numbers for radial basis function interpolation, Adv. Comput. Math., 1995, 3, 251–264.

Sgambi, L., Gkoumas, K. & Bontempi, F. (2012), Genetic algorithms for the dependability assurance in the design of a long span suspension bridge, *Computer-Aided Civil and Infrastructure Engineering*, 27(9), 655–675.

Stein, E.M. & Weiss, G. (1971), *Introduction to Fourier analysis on Euclidean space*. Princeton University Press, Princeton, N.J. USA.

Talebinejad, I., Fischer, C. & Ansari, F. (2011), Numerical evaluation of vibration based methods for damage assessment of cable stayed bridges, *Computer-Aided Civil and Infrastructure Engineering*, 26(3), 239–251.

Xia, Y., Ni, Y.Q., Zhang, P., Liao, W.Y. & Ko, J.M. (2011), Stress development of a super-tall structure during construction: numerical analysis and field monitoring verification, *Computer-Aided Civil and Infrastructure Engineering*, 26(7), 542–559.

Xiang, J. & Liang, M. (2012), Wavelet-based detection of beam cracks using modal shape and frequency measurements, *Computer-Aided Civil and Infrastructure Engineering*, 27(6) 439–454.